Knowledge-Based Systems 240 (2022) 108123

Contents lists available at ScienceDirect

Knowledge-Based Systems

journal homepage: www.elsevier.com/locate/knosys

Adaptive density peaks clustering: Towards exploratory EEG analysis

Tengfei Gao [a], Dan Chen [a,*], Yunbo Tang [a], Bo Du [a], Rajiv Ranjan [b], Albert Y. Zomaya [c], Schahram Dustdar [d]

[a] The School of Computer Science and the National Engineering Research Center for Multimedia Software, Wuhan University, Wuhan 430072, China
[b] The School of Computing, Newcastle University, Newcastle upon Tyne, NE4 5TG, United Kingdom of Great Britain and Northern Ireland
[c] The School of Information Technologies, the University of Sydney, Sydney, 2006, Australia
[d] The Distributed Systems Group (DSG) of Information Systems Institute, Vienna University of Technology, Vienna, 1040, Austria

ARTICLE INFO

Article history:
Received 19 July 2021
Received in revised form 3 October 2021
Accepted 1 January 2022
Available online 11 January 2022

Keywords:
Adaptive clustering
Exploratory data analysis
Density peaks clustering
EEG
Epileptic seizure

ABSTRACT

Finding appropriate *cluster centers* and determining the *scope of influence* explicitly associated with each center is at the very core of a successful clustering process, which has long been particularly difficult and important when handling bio-signals such as electroencephalography (EEG). Considering exploratory EEG analysis as a typical case, this study forms an adaptive density peaks clustering (ADPC) solution to the open problem based on the Density Peaks Clustering (DPC) algorithm. First, in order to optimize the cutoff distance (key parameter previously set manually) to adapt to various clustering tasks, an optimization function was constructed with the target dataset's uncertainty that can be solved by the extended Pattern Search Algorithm (PSA). Second, ADPC automatically constructs a set of cluster centers by jointly ranking the local density and relative distance, and then fine-tuning the set by balancing the intra-set independence and the tendency as a center against extra-set competitors from the perspective of each candidate. An exploratory EEG analysis framework was then fostered by centering on ADPC. Benchmarks on public datasets show the superiority of ADPC over its mainstream counterparts in terms of effectiveness and adaptability. The case study on epileptic EEG indicates that (1) the framework achieves averages on Precision, Recall, and F1-score of 100%, 92.46%, and 95.92%, respectively, in seizure detection involving no a priori information, and (2) the key observations revealed through clustering match the accepted conclusions well. Overall, ADPC enables automated clustering, which is well adaptive to exploratory EEG analysis.

© 2022 Elsevier B.V. All rights reserved.

1. Introduction

Clustering aims to organize data elements of a dataset into distinct clusters according to their resemblance through unsupervised learning of the intrinsic patterns (if any) of the dataset, which then enables exploration of the dynamics of the underlying (real or imagined) system on the basis of the observations [1]. Data elements in the same cluster are characterized by a similarity higher than those in different clusters [2]. Clustering is probably the most important and fundamental means of exploratory data analysis for finding intrinsic hidden information and patterns (if any) without the need for a priori knowledge, for example, to detect uncertain abnormal states from brain imaging data. Its capability of unsupervised learning has proven extremely useful in various fields such as signal processing, data mining and pattern recognition in general [3].

An exploratory analysis of electroencephalography (EEG) is a typical case. As the dominant means for examining cerebral electrical activities [4], EEG technologies have a wide range of applications in cognitive neuroscience, and the diagnosis of diseases such as epilepsy, schizophrenia, and autism [5]. Nowadays EEG-based neuroscience & engineering tasks still heavily demand onerous and highly skilled labeling. Decision making will otherwise be unreliable even with contemporary supervised and semi-supervised learning methods, such as mainstream EEG classification models [6,7]. Clustering holds the potential to explore brain dynamics especially malfunctions recorded in EEG without the need for labels or having to know all the potential problems/pathology of the subjects beforehand, that is, basically a priori knowledge about the observations (an EEG dataset) provided by experts [8].

The earliest clustering algorithms such as K-*means* simply rely on distance to make decision on clustering, which assign the cluster members to centers based on their minimum distances and find the most appropriate cluster centers optimization of an distance-based objective function [9]. Distance-based algorithms are the most widely applied benefiting from this simple principle,

* Corresponding author.
E-mail address: dan.chen@whu.edu.cn (D. Chen).

https://doi.org/10.1016/j.knosys.2022.108123
0950-7051/© 2022 Elsevier B.V. All rights reserved.

but they cannot adapt to nonspherical clusters as data elements are assigned to the nearest center [10].

Distribution-based algorithms such as the Gaussian Mixture Model (GMM) that utilize predefined probability distribution functions to reproduce data elements for adapting to various data distributions subsequently emerge [11]. The accuracy of clustering is subject to the capability of the trial probability in representing the data. The number of distribution functions must be set in advance similar to the number of cluster centers in K-means according to a priori knowledge [12].

Clusters are more likely to have arbitrary shapes. Density-based algorithms identify clusters in a data space with a contiguous region of high point density [13]. The DBSCAN algorithm and its variants can find appropriate cluster centers, but still require manually setting key density parameters (MinPoints and neighborhood radius) [14] to distinguish different density levels, which itself is an active research topic for selecting optimal parameters [15].

The advent of density peaks clustering (DPC) [16]marks the peak of these attempts. DPC has the advantages of both distance- and density-based methods, with the merits of identifying arbitrarily shaped clusters and their number without requiring explicit manual settings [17]. Although grand successes have been achieved with DPC and its variants [18] (see Section 2.1), challenges with adaptability still remain when handling data with no strong features or with intensive interferences such as bio-signals in practical applications. They are (1) unnecessary limits incurred by empirical setting of the key parameter (cutoff distance), and (2) difficulty in selecting the cluster centers.

However, it is not trivial even for a sophisticated clustering method to detect abnormalities and events from such bio-signals which are highly complex and nonstationary [19]. There is a pressing need for an alternative clustering method with adaptability that is significantly enhanced towards exploratory EEG analysis. This study utilizes advanced optimization theory in connection with the uncertainty of the target dataset to adaptively adjust the cutoff distance (d_c) as the key parameter in DPC directly influencing the accuracy of clustering. It may not necessarily fix the cluster centers at the beginning, as more evidence on decision making should be revealed in the course of clustering, especially in the case of multiple center candidates coexisting in a high-density region.

This study proposes an adaptive density peaks clustering approach (ADPC) by extending the DPC algorithm (Section 3):

1. Adaptive selection of the cutoff distance. To obtain the optimal cutoff distance for adapting to various clustering tasks, an optimization function was constructed using the Gini index to measure the uncertainty of the target dataset. Then, the extended pattern search algorithm (PSA) with global optimization capability was applied to obtain the optimal cutoff distance value.
2. Automatic determination of cluster centers. To avoid bias in the manual determination of cluster centers, ADPC automatically constructs a set of cluster centers by jointly ranking the local density and relative distance (measure γ) and then fine-tuning the set by balancing the intra-set independence and the tendency as a center against extra-set competitors from the perspective of each candidate. Once the extra-set competitor holds the tendency as a center, the corresponding data point is filled in, and the corresponding candidate with relatively low independence is filtered out.

A generic framework for exploratory EEG analysis has been fostered by centering on the ADPC approach combining discrete Fourier transform (DFT) and Bayesian factorization (Section 4). The design aims at automatic clustering in the course of exploring the target. Thus, blind exploration of brain malfunctions may be possible without the need for excessive a priori information.

Benchmark experiments on public clustering datasets were performed to evaluate the adaptive capability and the accuracy of ADPC against relevant counterparts in clustering tasks (Section 5). A case study on epileptic EEG was carried out to evaluate the proposed framework in terms of the capability of exploratory analysis (Section 6).

The main contributions of this study are as follows:

1. This study develops an adaptive clustering approach by extending the DPC algorithm that can optimize the key parameters and determine the cluster centers by itself. It enables adaptive clustering with fully automated operation based on the target dataset without the need for human intervention or empirical setting of key parameters. The resulting algorithm significantly outperforms the mainstream counterparts.
2. A clustering-based framework for exploratory EEG analysis is provided aiming at pathological EEG, and it is proved to be effective for seizure detection. It holds the potential to find abnormal neural activities from EEG without explicit a priori knowledge of the subjects under examination as the classification models do.

2. Related work

Existing clustering algorithms can be based on metrics such as distance, distribution, density, or their combinations. Extensive and comprehensive literature reviews of research exist along this direction [20,21]. This section then focuses on the family of DPC and the most salient EEG clustering methods, as they are closely related to this study.

2.1. Density peak clustering family

DPC algorithm excels in detecting arbitrary shaped clusters and determines the cluster centers in a heuristic way [16,22]. DPC assumes that cluster center is a point with a higher local density compared with its surrounding neighbors and it is located at a relatively large distance from any other points with a higher local density. Recent DPC variants largely aim to tackle the pitfalls empirical setting of the cutoff distance d_c and manual determination of cluster centers [23].

Du et al. proposed the DPC-KNN algorithm incorporating k-nearest neighbors in local density computation [24], which might reduce the risk of incorrect clustering by d_c. The DPC-KNN still needed to know the number of the nearest neighbors beforehand. Jiang et al. have developed the GDPC algorithm based on the gravitation theory to accurately identify centroids and anomalies, which attempts to exclude the influence of d_c on the clustering results [25]. Both methods left cluster centers manually determined via Decision Graph.

Wang et al. proposed to determine the number of clusters prior to clustering by finding the "knee point" as the boundary between a cluster center and a noncluster center [26], and the knee point could be derived by minimizing the root mean squared error of two fitting curves. Bie et al. have also developed a method (fuzzy-CFSFDP) to select the cluster centers aided by fuzzy theory raised from statistical analysis against local density and relative distance of cluster centers conforming to Gaussian distribution [27]. Both methods can effectively handle synthetic data but leave the situation of multiple cluster centers co-existing in a high-density region unattended.

2.2. EEG clustering

Existing EEG clustering methods focus on feature engineering tasks such as feature selection, feature extraction, and/or grouping of EEG epochs of different states.

Alshebeili et al. have enabled seizure prediction based on K-means with a high performance in terms of prediction accuracy and false alarm rate [28]. Based on the statistical characteristics of amplitude, median, mean, variance and derivative of EEG, K-means could complete the task of seizure prediction with a performance comparable to multilayer perception (MLP) networks.

Bizopoulos et al. have also developed a method to detect the epileptic seizures using K-means and Ensemble Empirical Mode Decomposition (EEMD) [29]. Marginal Spectrum (*MS*) obtained via EEMD formed the basis for clustering by K-means without the need for training data.

Paolo et al. proposed to use a fuzzy clustering method to sustain workflow for EEG event-related potentials [4]. Fuzzy clustering worked in the very core to grade the weighted feature vectors in clustering. Experimental results of emotional Go/NoGo task show the method's robustness to artifacts.

As a contrast to the above, this study is intended to bridge the gap between the most advanced clustering algorithm and the open problems complicated in exploratory analysis of bio-signals. The major concerns include (1) how to automatically optimize the key parameters and determine the cluster centers adapting to various datasets and (2) how to enable an effective method of exploratory EEG analysis.

3. Adaptive density peak clustering

This section first covers the background of the DPC method and notations referenced throughout the following discussions. The design of the adaptive DPC is then given. In particular, the basic theories of the ADPC algorithm are detailed, including: (1) adaptive selection of cutoff distance, (2) automatic determination of cluster centers and, (3) complexity analysis.

3.1. Background and notations

For a given dataset $S = \{x_1, x_2, \ldots, x_N\}$, let $I_S = \{1, 2, \ldots, N\}$ represent its corresponding index set. A certain distance between data points x_i and x_j in S, such as the Euclidean distance, is denoted by $d_{ij} = dist(x_i, x_j)$. In the context of the DPC algorithm, the *local density* ρ_i of data point x_i, similar to *MinPoints* in DBSCAN, is defined as follows:

With the assumption of discrete data elements, the local density ρ_i can be defined as (1).

$$\rho_i = \sum_j \chi(d_{ij} - d_c), \tag{1}$$

where $\{i, j | i \neq j\} \in I_S$, and the function $\chi(x)$ is defined as (2):

$$\chi(x) = \begin{cases} 1, x < 0 \\ 0, x \geqslant 0. \end{cases} \tag{2}$$

When continuous data are assumed, the local density can be alternatively defined as (3):

$$\rho_i = \sum_j e^{-(\frac{d_{ij}}{d_c})^2}, \tag{3}$$

where d_c is the only parameter to be manually set in the DPC and defines the *scope of influence* of each data element/point. The cutoff distance d_c plays an important role in computing the local density ρ_i. As shown in Fig. 1, ρ_i indicates the number of data points in the influence scope confined by d_c. The accuracy of clustering depends heavily on the setting of d_c.

The DPC algorithm empirically sets d_c to ensure that the average number of neighbors is approximately 1%–2% of the total number of data points in the dataset. This setting aims to gain adaptability, but the appropriate d_c for various problem domains may differ. Note that feature extraction or alike can alleviate the high complexity and nonstationarity embedded in the data under examination, and the direct application of DPC can still be risky, as the range of d_c remains unclear. The success of clustering in this context is subject to the appropriate, that is, adaptive to the dataset, setting of d_c. The capability of adaptively setting an appropriate d_c is desired to adapt to the corresponding problem domain.

Data field depicts the interactions between objects (i.e., other data points) associated to each data point in the whole data space, mimicking the field theory in physics [30]. In this context, individual data point radiate their strengths (measurements of influence) and vice versa. The local density ρ_i is defined the difference in focusing on each individual data point. The data field theory is then applied in designing the adaptive DPC.

For data point x_i, the *relative distance* δ_i is defined as (4):

$$\delta_i = \begin{cases} \min\limits_{j:\rho_j > \rho_i} (d_{ij}), \ \rho_i < \max\limits_k(\rho_k), \\ \max\limits_j(d_{ij}), \ \rho_i = \max\limits_k(\rho_k). \end{cases} \tag{4}$$

Relative distance δ_i is measured by computing the minimum distance between data point x_i and any other data points with higher density. However, for the data point with the highest local density, δ_i takes the maximum distance to all other points.

As shown in Fig. 1, data point 14 is closest to data point 12 among the first 13 points with higher density, such that $\delta_{14} = d_{(14,12)}$ and the relative distance of data point 1 is $d_{(1,27)}$, which is the maximum distance from data point 1 to the rest of the data points. *Cluster centers* are recognized as points for which the value of ρ_i and δ_i are anomalously large, and the Decision Graph is constructed based on ρ_i and δ_i to identify cluster centers. The remaining data points are then allocated to the same clusters as their nearest neighbors of higher density. As shown in Fig. 1, the areas within the blue and red dashed lines represent the scope of influence explicitly associated with centers 1 and 10, respectively, and the scope of center 10 is equal to its influence area with d_c.

Moreover, for each cluster, the set of data points assigned to it but also located within a distance d_c from the data points belonging to other clusters form a *border region*, and the maximum local density within its border region is denoted as ρ_{max}. The data points with a density higher than ρ_{max} are considered as *cluster cores*; otherwise, they are regarded as cluster halos, that is, *noise*, which are more likely.

Pattern Search Algorithm (PSA) aims to solve the optimization problem of functions that are difficult to derive [31]. This study extends this to solve the optimization function constructed by measuring the *uncertainty* of the target dataset (Section 3.2.1). This metric reflects the chaotic state of the potential distribution of the dataset and can be measured using the *Gini* index:

$$Gini = 1 - \sum_{i=1}^{c} (p_i)^2, \tag{5}$$

where p_i is the probability that the data points belong to the ith category, and c is the number of categories.

Let $\Phi_i = \varphi(x_i)$ denote the potential value of the data point x_i. The relationship among the uncertainty, potential distribution, and Gini index is detailed in Section 3.2.1.

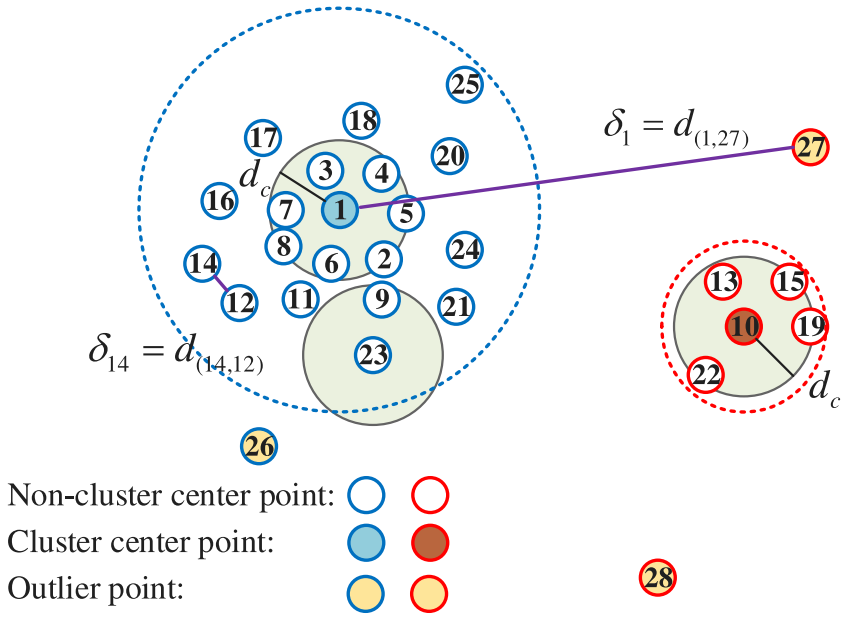

Fig. 1. Data point distribution. Data points are ranked in order of decreasing density and d_c is the radius of the influence area of data points. When the cutoff distance d_c is too large, such as $d_c \geqslant \max(d_{ij})$, all ρ_i are the same, and all the data points will be identified as one cluster. On the contrary, when the cutoff distance is too small, such as $d_c \leqslant \min(d_{ij})$, all the data points will be regarded as the cluster centers and divided into a single cluster. Data points 26, 27, and 28 have a relatively high δ and a low ρ, each considered as an individual *cluster* consisting of a single data point, i.e., an *outlier*.

To automatically determine cluster centers, the metric γ is proposed to jointly consider ρ and δ [16] as defined in (6):

$$\gamma_i = \rho_i \delta_i, \tag{6}$$

γ_i is sorted in descending order to obtain the γ sequence ($\{seq(\gamma_i)\}_{i=1}^{N}$). Furthermore, the γ of the *cluster center point* nearest to the *noncluster center point* in the γ sequence is expressed as: γ_{BD}. Meanwhile, the noncluster center point with the γ value closest to γ_{BD} is treated as a *competitor*. The difference between candidates in the γ sequence can be viewed as the *independence* in the set of center candidates to be adjusted. The *tendency* of a candidate to be identified as a cluster should be measured to screen out unqualified candidates (see Section 3.2.2).

3.2. Design and theories of adaptive density peak clustering

This study complements the DPC method with the innovations of adaptively selecting the optimal cutoff distance and automatically determining the appropriate cluster centers. The resulted algorithm of ADPC is described in Algorithm 1.

To tackle the pitfall of the empirical setting of the cutoff distance, ADPC introduces data field theory to adaptively obtain the optimal cutoff distance $\widehat{d_c}$ by constructing an optimization function with the Gini index and then using the extended PSA to drive the function to the optimum. To enable automatic determination of appropriate cluster centers instead of resorting to experts' visual inspection as DPC does, ADPC constructs a set of cluster centers by ranking the γ and fine-tuning the set based on the *independence* and *tendency* of cluster center candidates. The pillar theories proposed in ADPC are described in Sections 3.2.1 and 3.2.2 respectively.

3.2.1. ADPC: Selection of cutoff distance

The data field theory is introduced here to adaptively obtain the optimal cutoff distance $\widehat{d_c}$ value based on the interactions of data points by fully considering the overall distribution especially the potential value representing the interaction dynamics

Algorithm 1 Adaptive Density Peak Clustering

Input:
Distance matrix: D.
Output:
Cluster result: C.

1: Sort d_{ij} in a ascending order;
2: Set d_c be the value of 2% position in the above order;
3: Selection of cutoff distance module:
- Use the extended PSA to solve (11) to obtain $\widehat{d_c}$.

4: Calculate ρ_i and δ_i based on (1) or (3), and (4), respectively;
5: Determination of cluster centers module:
- Construct the set of cluster centers by jointly ranking the local density and relative distance (measure γ) with using (6) and (15).
- Fine-tune the set by balancing the intra-set independence and the tendency as a center against extra-set competitors from the perspective of each candidate with using (16) and (17).

6: Allocate remaining points to the same cluster as its nearest neighbor of higher density.
7: Identify border regions to distinguish cluster cores and cluster halos.

of objects (data points). The distribution of the data field can be described as a potential function, and the potential value of an arbitrary point $x_i \in \Omega (i = 1, 2, \ldots, n)$ in the data field is defined as (7):

$$\varphi(x_i) = \sum_{j=1}^{n} (m_j \times K(\frac{\|x_i - x_j\|}{\sigma})), \tag{7}$$

where m_j ($m_j \geqslant 0, \sum_{j=1}^{n} m_j = 1$) is the mass of x_j and it represents the strength of the data field from x_i, $\|x_i - x_j\|$ is the distance between point x_i and point x_j, σ is an impact factor

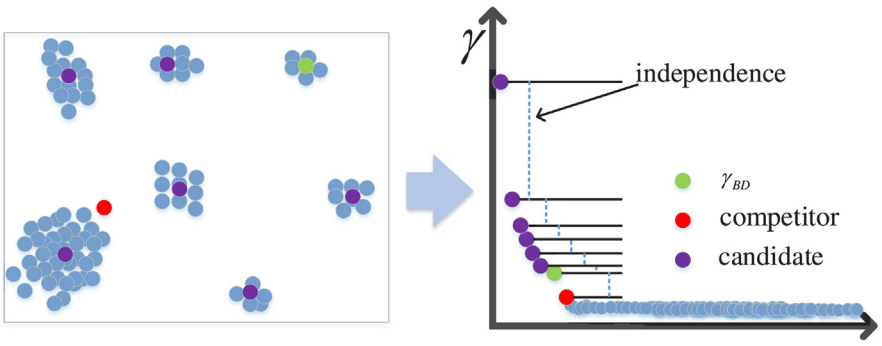

Fig. 2. γ is ranked in descending order to construct set of cluster center candidates.

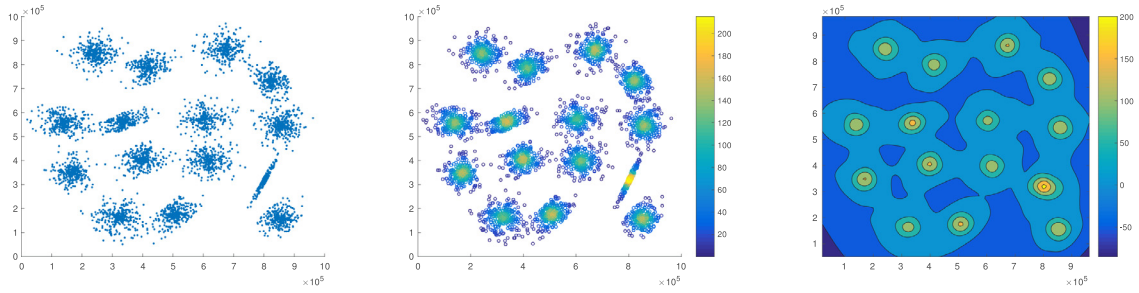

(a) The true distribution of original dataset (b) The local density distribution of the original dataset (c) The potential distribution of the original dataset

Fig. 3. Both local density and potential can match the distribution of original dataset.

that controls the interaction distance between points, and $K(x)$ is a unit potential function. Clearly, the potential function directly measures the density of data distribution. The potential is strong in a data-intensive area and weak in a data-sparse area [32].

$K(x)$ is assumed to be a Gaussian kernel function as it is ubiquitous and well matches the data nature of the data field [33]. The Gaussian potential of point x_i is defined as (8):

$$\varphi(x_i) = \sum_{j=1}^{n}(e^{-(\frac{\|x_i - x_j\|}{\sigma})^2}), \tag{8}$$

The definition of ρ_i is similar to the Gaussian potential of point x_i. As shown in Fig. 3, both the local density and potential match the distribution of original dataset. The distribution of the potential value is determined by impact factor σ, as the local density is determined by d_c. Hence, the optimal value of d_c can be solved in the same manner as the optimal σ.

The Gini index measures the uncertainty of systems associated with random variables and is positively related to uncertainty. For a data field, the Gini index (defined as (9)) measures degree of uncertainty, that is, how nonstationary the dataset under examination is. When the potential values of all data points are the same, the corresponding uncertainty reaches its maximum with the greatest Gini index obtained; in contrast, the smallest Gini index denotes that the data field is the most unbalanced and clustering of the dataset should be the most straightforward.

$$Gini = 1 - \sum_{i=1}^{n}(\frac{\Phi_i}{\sum_{i=1}^{n}\Phi_i})^2. \tag{9}$$

The Gini index then manifests a nonlinear univariate function with impact factor σ, and the optimal σ can be obtained when the Gini index is minimized. The potential distribution of the data field is then said to best match its distribution [34]. Therefore, the objective function with respect to the impact factor σ can be denoted as (10):

$$\widehat{\sigma} = arg\min_{\sigma}(Gini(\sigma) = 1 - \sum_{i=1}^{n}(\frac{\Phi_i(\sigma)}{\sum_{i=1}^{n}\Phi_i(\sigma)})^2). \tag{10}$$

The objective function of the cutoff distance d_c can be obtained as (11). Clearly, the optimal value of d_c is the same as that of σ.

$$\widehat{d_c} = arg\min_{d_c}(Gini(d_c) = 1 - \sum_{i=1}^{n}(\frac{\rho_i(d_c)}{\sum_{i=1}^{n}\rho_i(d_c)})^2). \tag{11}$$

Obviously, the solution of (11) has a fair initialization that is to the optimal cutoff distance $\hat{d}_c$ when the initialization is set to the first 1%–2% of the d_{ij} sequence [16]. ADPC extends the PSA to derive a solution to this optimization problem, which iteratively drives the objective function to the optimum. The conventional PSA decides (in the current step x_k) the direction of the next search (step x_{k+1}) only in comparison with the value of the objective function in the current step, that is $(f(x_{k+1}), f(x_k))$, which may result in premature convergence. The improved algorithm then refers to m ($m > 1$) steps to reduce the risk of falling in the local optimum: $(f(x_{k+1}), maxf(x_{k-m}), f(x_{k-m+1}), \ldots, f(x_k))$. Therefore, the rule of step 2 in Algorithm 2 is changed to:

$$f(y_j \pm de_j) < \max_{max(k-m,0)\leqslant j\leqslant k} f(y_j). \tag{12}$$

When m = 0, it degenerates into the original comparison method.

The main purpose of introducing an extended PSA is to quickly search $min(Gini)$ and the corresponding $\widehat{d_c}$, which makes the search more efficient than the traversal method. Although some extra hyperparameters have been introduced, their effect on the final clustering results is much lower than that of d_c. Among them, only the acceleration and contraction coefficients can directly influence the search process speed. For the comparison

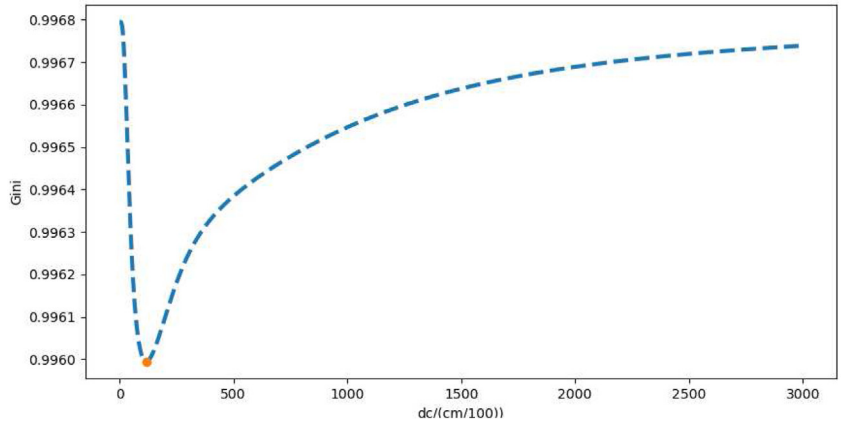

Fig. 4. The trend of Gini with different cutoff distance in dataset Spiral.

Algorithm 2 Extended Pattern Search Algorithm

Input: Acceleration coefficient $\kappa \geqslant 1$, contraction coefficient $\beta \in (0, 1)$, convergence coefficient $\varepsilon > 0$, initial step-size d, ($d > \varepsilon$).

Output: Optimal solution: x_k.

1: Set the initial value $x_1 \in R^n$ and set $y_1 = x_1$, $k = 1$, $j = 1$;
2: The axial search:
if $f(y_j + de_j) < \max_{max(k-m,0)\leqslant j\leqslant k} f(y_j)$
$y_{j+1} = y_j + de_j$, turn to step 3;
else if $f(y_j - de_j) < \max_{max(k-m,0)\leqslant j\leqslant k} f(y_j)$
$y_{j+1} = y_j - de_j$, turn to step 3;
else set $y_{j+1} = y_j$;
3: if ($j < n$)
$j := j + 1$, turn to step 2.
if ($f(y_{n+1}) < f(x_k)$)
turn to step 4;
else turn to step 5;
4: The pattern search:
set $x_{k+1} = y_{n+1}$, $y_1 = x_{k+1} + \kappa(x_{k+1} - x_k)$.
$k := k + 1$, $j = 1$ and turn to step 2.
5: if ($d \leqslant \varepsilon$)
End the search and output point x_k;
else
Set $d = \beta d$, $y_1 = x_k$, $x_{k+1} = x_k$.
Set $k := k + 1$, $j = 1$ and turn to step 2.

factor, setting it to be a smaller integer (i.e., 1,2,3) is less difficult and influential than the direct setting of the original d_c. As shown in Fig. 4, there is only one extremum of *Gini*, at which the comparison coefficient m has little influence. Overall, these hyper-parameters introduced are easier to set and have a lower direct impact on the results.

3.2.2. ADPC: Determination of cluster centers

The DPC requires visual inspection of the Decision Graph to manually set the cluster centers. This is particularly risky when handling complex Decision Graphs grows complex. For example in Fig. 5, difficult to determine whether the data points in the circles can be identified as cluster centers. This also complicates scenarios in which human participation does not apply or becomes difficult. ADPC then aims to automatically determine accurate cluster centers based on the dataset itself without the need for manual operations. The DPC selects cluster centers from data points with large ρ and δ, that is, a large γ. Following

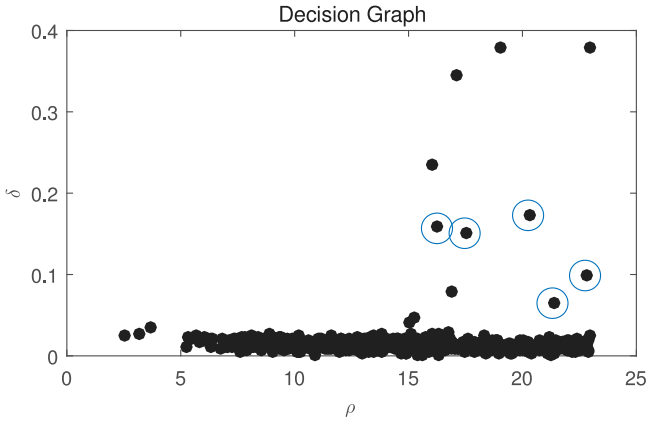

Fig. 5. An instance of decision graph.

this loose principle, the key issue is to find the boundary (γ_{BD}) between the cluster center point (γ_{Cc}) and the noncluster center point (γ_i).

Ranking γ_i of all data points in descending order, as shown in Fig. 2, most of the γ_is concentrate on a low value, while those of few data points are large. For noncluster center points (approximately indexed 7 onward), the average value $\hat{\gamma}$ is close to γ_i in the middle, and their γ_is descend almost linearly and slowly. When viewing the γ values of data points through the boundary point (γ_{BD}) to a cluster center point (γ_{Cc}), there exists a jumping point with γ. This observation provides a clue for identifying γ_{BD} by scanning the γ sequence. The consecutive Z (odd positive) γs are selected from $\{seq(\gamma_i)\}_{i=1}^{N}$: $\{seq(\gamma_j)\} = \{seq(\gamma_j), seq(\gamma_{(j+1)}), \ldots, seq(\gamma_{(j+Z-1)})\}$, and the mean value of $\{seq(\gamma_j)\}$ can be obtained:

$$\overline{\{seq(\gamma_j)\}} = \frac{\sum_{j\in\{1,(N-Z)\},k=0}^{Z} seq(\gamma_{j+k-1})}{Z}. \tag{13}$$

The γs of noncluster center data points can be expressed as formula Eq. (14):

$$\overline{\{seq(\gamma_j)\}} \approx seq(\gamma_{(j+(Z-1)/2)}). \tag{14}$$

Consequently, the following formula can be obtained to determine whether $\{seq(\gamma_j)\}$ satisfies the linear trend:

$$\left|\overline{\{seq(\gamma_j)\}} - seq(\gamma_{(j+(Z-1)/2)})\right| \leqslant \xi, \tag{15}$$

where ξ is a small positive value. For the sequence $\{seq(\gamma_j)\}$, there are two moving methods, forward and backward, to scan $\{seq(\gamma_i)\}_{i=1}^{N}$ to find γ_{BD}.

When using the forward moving method, sequence $\{seq(\gamma_j)\}$ is constructed from γ_0 and moves forward one point each time. In each movement, we observe whether the sequence $\{seq(\gamma_j)\}$ satisfies in formula (15). Once sequence $\{seq(\gamma_j)\}$ satisfies the above inequality relationship, the movement stops and the γ_j in $\{seq(\gamma_j)\}$ is regard as the γ_{BD}.

When using the backward moving method, sequence $\{seq(\gamma_j)\}$ is constructed from γ_q, which is in the middle of $\{seq(\gamma_i)\}_{i=1}^{N}$ and moves backward by one point each time. Similarly, we observe whether the sequence $\{seq(\gamma_j)\}$ satisfies the linear trend in each movement. On the contrary, it satisfies the inequality relation at the early stage of backward movement. Therefore, when the sequence $\{seq(\gamma_j)\}$ does not satisfy the inequality relation for the first time, the corresponding γ_j in $\{seq(\gamma_j)\}$ is regard as γ_{BD}. After finding γ_{BD}, the data points satisfying $\gamma_i \geqslant \gamma_{BD}$ are considered as candidate cluster centers. Then the set of cluster center candidates is constructed for fine-tuning.

It is worth noting that the value of γ_q can be set to the first 50% point of $\{seq(\gamma_i)\}_{i=1}^{N}$. The reason for this setting instead of starting from the last point is for fewer movements and comparisons. Under normal circumstances, the number of clusters in the data set is not very large, so there is a small probability to cause the omission of cluster centers. Meanwhile, this setting is not mandatory, and γ_q can also be located further back in $\{seq(\gamma_i)\}_{i=1}^{N}$.

In addition, parameter Z determines the length of $\{seq(\gamma_j)\}$ and can be set to an odd number above 3 (e.g. 5,7). Different ways of moving correspond to different ways of setting. When using the forward moving method, Z can set to slightly larger to reduce the risk of ending the movement early when $\{seq(\gamma_i)\}_{i=1}^{N}$ corresponding to the dataset with many true cluster centers showing a downward linear trend before γ_{BD}. When using the backward moving method, a slightly smaller Z will be more suitable, because it can reduce the risk of a small jump at the γ_{BD} resulting in a small $\{\overline{seq(\gamma_j)}\}$ value transformation and then continue looking forward for γ_{BD}. Even if Z is not set appropriately, which results in the inaccuracy of the candidate set, the subsequent fine-tuning process will corrects this to ensure that an accurate cluster center is obtained.

Fine-tuning checks extra-set competitors against intra-set candidates in terms of *independence*. Given L candidates in the initial set, the difference in γ between the jth data point and its rightward neighbor is D_j; the average value of D among the candidates is D_μ.

Starting from the Lth D, ADPC compares D_j $(j > L)$ with D_μ in order: Once $D_j \geqslant D_\mu$ is satisfied, the competitor will be filled into the candidate set and D_μ updates; the number of comparisons to be made, T, can be set to 5. Next, the ADPC filters out the unqualified candidates based on the *tendency*. According to the fundamental assumption of cluster centers regarding relative distance, their values are much larger than the cutoff distance d_c, which are said to conform to the restriction:

$$\delta_{Cc} \geqslant d_c. \tag{16}$$

Moreover, when there are multiple center candidates in a region with high density, they are usually very close to each other. Therefore, it is necessary to determine whether these center candidates can be identified as the final independent cluster centers, which determines whether the clusters after subsequent allocation should be merged or separated. Thus, all cluster centers complete the screening process by comparing the cutoff distance and the shortest distance ($dist_{min}$) of the center candidates. When $dist_{min}$ is less than d_c, the center candidate is filtered out. Thus, all the candidates satisfy (17).

$$dist_{min} > d_c. \tag{17}$$

Ultimately, the final actual cluster centers are determined accurately from the set of candidates using the fine-tuning process.

3.2.3. Complexity analysis

Suppose that the dataset contains n data points and let C denote the number of clusters. In the process of ADPC, there are three main parts that require storage spaces: first, the distance matrix needs space to store and the space complexity is $O(n^2)$. Second, ADPC needs space to store d_{ij}, which is $c_1 n^2$ entries, where c_1 represents a constant. Third, each point has four attributes: ρ, δ, *Gini*, and γ, which need $4n$ spaces. Thus, the overall space complexity of ADPC is $O(n^2)$. As for DPC, the distance matrix and the two attributes (ρ and δ) of each point need to be stored, while the value of d_c is only an entry. Furthermore, as an improved algorithm of DPC, the space required by DPC-KNN [24] includes three parts. The first two parts are consistent with DPC, and the latter part, which is used to store d_{ij}, is the same as the second part of the ADPC. Thus, the overall space complexity of the three algorithms can be written as $O(n^2)$.

The time complexity of ADPC is mainly derived from the following five aspects: (a1) the time complexity for computing ρ, δ and *Gini* for each data point i are all $O(n^2)$, and (a2) the time complexity of the extended PSA algorithm is $O(log(n))$. Therefore, the time complexity of obtaining $\widehat{d_c}$ is $O(n^2 log(n))$. (a3) The time complexity of d_{ij} and γ depends on the sorting algorithm, the minimum $O(nlog(n))$, and the maximum $O(n^2)$, so the total complexity of this aspect does not exceed $O(n^2)$; (a4) the time complexity of fine-tuning in the determination of the cluster center module is $O(n)$, and (a5) the time complexity in the data point allocation process is $O(C * n)$. Therefore, the overall time complexity of ADPC is $O(n^2 log(n))$.

Compared with ADPC, the time complexity of DPC involves two aspects: (b1) the time complexity for computing ρ and δ, and (b2) the time complexity in the data point allocation process. In addition to (b1) and (b2), DPC-KNN still has the same time complexity (a3) for finding the k-nearest neighbors by sorting. As for determining the cluster centers, this does not apply to the manual operations for DPC and DPC-KNN. The overall time complexity for the both is $O(n^2)$. The ADPC has an overhead in solving (11), whereas DPC and DPC-KNN are not involved, but this is obviously tolerable.

4. EEG exploratory analysis framework

A framework for exploratory EEG analysis was then designed based on ADPC, to find abnormal neural activities from pathological EEG without explicit a priori knowledge of the subjects under examination as the available to classification models. Fig. 6 provides an overview of the framework, which consists of three major modules: (1) time–frequency transformation with DFT, (2) EEG feature extraction with the Bayesian factorization approach (BF), and (3) clustering of EEG states.

EEG is first evenly segmented into a sequence of EEG epochs or *samples* in the context of machine learning; Spectrum information of the EEG samples is obtained via DFT; The resulted EEG tensor (three dimensions of *sample-channel-frequency*) is then factorized via BF to extract factor features; The distance matrix of the features forms the inputs for ADPC.

4.1. Extraction of EEG factor features

The framework first performs time–frequency transformation to EEG samples and obtains the frequency information with the Hamming window applied to avoid truncation. The EEG tensor is then formed with latent features extracted by BF, which excels with the merit of no demand for sufficient a priori knowledge of

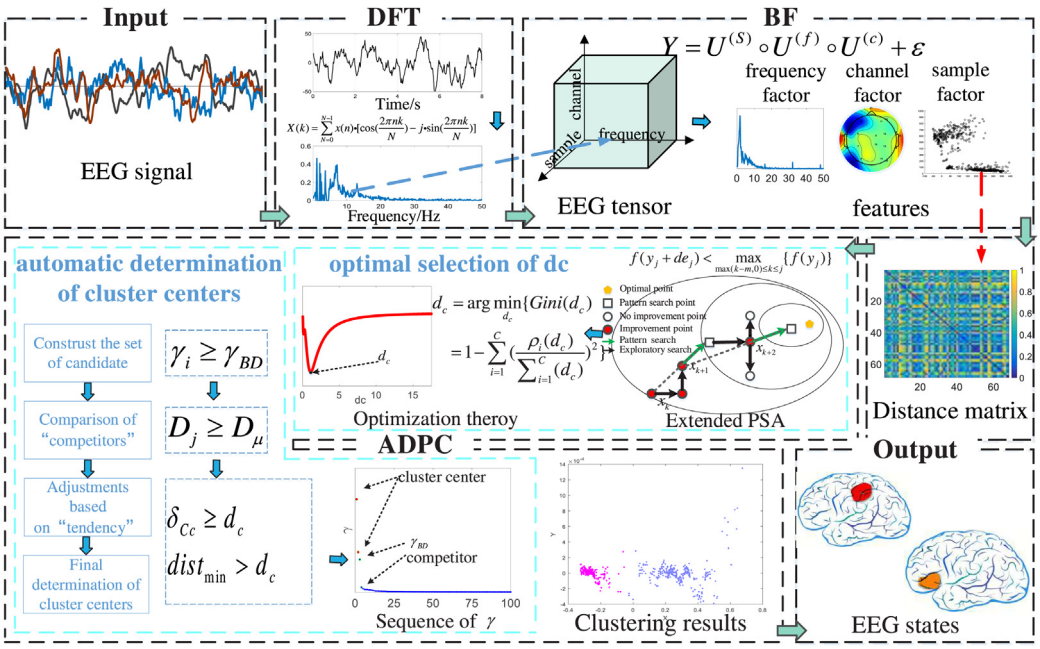

Fig. 6. Framework for ADPC-based EEG clustering analysis.

the problem domain and the capability to shift the most informative factors of EEG. The linear model for tensor decomposition is expressed as follows:

$$Y = X + \epsilon,$$
$$X = \sum_{r=1}^{R} U_r^{(1)} \circ \cdots \circ U_r^{(N)}, \tag{18}$$

where Y is the N-order tensor of size $I_1 \times \ldots \times I_N$, composed of the true tensor X and the noise tensor ϵ. $U^{(n)}(1 \leqslant n \leqslant N)$ represents the n-mode factor matrix of size $I_n \times R$ with the rth column $U_r^{(n)}$ and the positive integer R is referred to as the tensor's *rank*. The operator $\circ$ denotes the *outer product*.

BF assumes non-informative priori of the factor vector $\mathbf{U}_{\mathbf{i_n}}^{(\mathbf{n})}(1 \leqslant n \leqslant N, 1 \leqslant i_n \leqslant I_n)$, the i_nth row of factor matrix $U^{(n)}$ and each element in noise tensor ϵ both conform to i.i.d. Gaussian distribution. The probabilistic model adapts an approximate inference under the variational Bayesian framework for the posterior distribution. Then the posterior distribution of the factor matrix is obtained when the lower bound of marginal likelihood $p(Y)$ is maximized and the factor matrices for all modes are obtained by the mean of posterior distributions [35].

4.2. Clustering EEG states

ADPC-based state recognition is at the core of the framework. Taking 3-order tensor (sample-channel-frequency) as an example, the most significant features obtained by the BF approach are depicted in the modes of the sample, frequency and channel. The factor matrix of sample mode $U^{(s)}$ includes the dissimilarity among the EEG data samples. Clustering the factor features of the EEG sample mode holds the power to explore and identify the pathological states of the brain's cerebral electrophysiological activities. ADPC is applied for grouping EEG states from low-dimensional sample factors. The distance matrix of the sample features is calculated to be the input of the ADPC and the clustering results obtained can be used for exploratory analysis of pathological EEG. The detected abnormalities may then be concentrated for further examination with more sophisticated analytics in neuroscience and engineering tasks.

Table 1
Public synthetic datasets.

Dataset	Records	Clusters	Source
Flame	240	2	[36]
Spiral	312	3	[37]
R15	600	15	[38]
Aggregation	788	7	[39]
S1	5000	15	[40]
Unbalance	6500	8	[41]

5. Performance evaluation

This study performed benchmarks of ADPC on public datasets against the mainstream counterparts. The testbed for the experiments was a PC equipped with CPU (Intel (R) i5-7500@3.4 GHz), RAM (16 GB), and OS (Windows 10).

Benchmarks were intended to test the capability of ADPC to recognize clusters of arbitrary shapes on the public datasets available at http://cs.uef.fi/sipu/datasets/. Table 1 described the details of these synthetic datasets significantly varying from each other in size and number of clusters. Four state-of-the-art clustering algorithms were checked against three types: (1) classic clustering: K-means and DBSCAN, (2) the original DPC algorithm, and (3) the improved DPC algorithm: DPC-KNN [24]. The Euclidean distance was used to calculate the distance in the clustering process for all algorithms.

The performance of these clustering algorithms was evaluated using two widely applied metrics: the adjusted rand index (ARI) and adjusted mutual information (AMI).

- *ARI* could be regard as a modified metrics of Rand index (RI) with higher discrimination. The value ranges of ARI and AMI are both $[-1,1]$, and the larger ARI-implied clustering results were more consistent with the real data distribution:

$$ARI = \frac{RI - E(RI)}{max(RI) - E(RI)}. \tag{19}$$

Table 2
Parameters setting of algorithms.

Dataset	K-means	DBSCAN	DPC-KNN
Flame	k = 2	eps = 1.56, MinPoints = 14	p = 1.0%
Spiral	k = 3	eps = 1.20, MinPoints = 2	p = 2.5%
R15	k = 15	eps = 0.40, MinPoints = 10	p = 0.5%
Aggregation	k = 7	eps = 1.50, MinPoints = 9	p = 1.0%
S1	k = 15	eps = 0.04, MinPoints = 26	p = 1.0%
Unbalance	k = 8	eps = 0.03, MinPoints = 8	p = 1.0%

- *AMI* measured the degree of the consistency between data distributions based on the Mutual Information theory:

$$AMI = \frac{MI - E(MI)}{max(H(U), H(V)) - E(MI)}. \quad (20)$$

Suppose U and V are two distributions of N sample labels, then $H(U)$ and $H(V)$ are the entropies of the two distributions, respectively; MI is the mutual information between U and V. The value range of AMI is also $[-1,1]$, and a larger AMI indicated that the clustering results were more consistent with the real labels.

DPC and DPC-KNN both set d_c to 2% of d_{ij} in the dataset. ADPC sets the parameters of extended PSA in the process of clustering: acceleration coefficient $\kappa = 2$, contraction coefficient $\beta = 0.5$ and comparison coefficient m = 3. The search initialization and initial step size were set to 2% and 0.1% of d_{ij}, respectively. In addition, Table 2 presents the details of the K-means, DBSCAN and DPC-KNN remaining relevant parameter settings.

Table 3 presented the benchmark results of the clustering algorithms in terms of ARI and AMI. All results were averaged across 20 iterative trials. The results indicated that:

- All algorithms performed well on datasets R15, S1, and Unbalance. This was also the case on Flame, Spiral, and Aggregation data sets (except K-means).
- ADPC, DBSCAN, and DPC-KNN outperformed DPC and K-means on Spiral dataset; ADPC's AMI and ARI values on Flame, Spiral, and Aggregation datasets were all 1.
- ADPC outperformed DPC on all datasets except the Unbalance dataset.

The performance of DPC-KNN was close to that of ADPC, but its key parameter k should be set manually beforehand, where k is computed as a percentage (p) of the number of data points N, so $k = p \times N$. This parameter significantly influenced the performance of DPC-KNN, and no solution to automating the setting was available but enumeration verification.

Fig. 7 presented the clustering results of ADPC in 2D scaling. The main observations from the results were as the follows:

- ADPC efficiently aggregated typical shape datasets (Flame, Spiral, and Aggregation), even though Spiral dataset brought challenges to the most clustering algorithms owing to its nonspherical shape. ADPC holds the potential to adapt to arbitrary shape clustering tasks.
- ADPC accurately identified the real clusters of all datasets, although the number of clusters was different. There were more than two clusters in all datasets except the Flame dataset, and the number of clusters in the R15 and S1 datasets were both 15. ADPC excelled in finding the correct number of clusters.
- The above datasets were of various sizes, and the performance of ADPC was not sensitive to the sizes at all.

6. Case study: Epileptic EEG exploration

The case study examined the potential of the ADPC-based framework to explore the malfunctional brain dynamics recorded in pathological EEG, without sufficient background information about the observations, that is, the exact problems with the subjects. It explored an epileptic EEG dataset to evaluate the effectiveness of singling out epileptic seizures, and these unpredictable and rare occurrences of electrical discharges in a focal area or the entire brain were very meaningful in the monitoring and diagnosis of epilepsy patients. The case study consisted of three stages: (1) *blind exploration*, (2) *examination of abnormalities*, and (3) *verification*.

This case study begins with *blind exploration*, which should complete the clustering-related task of blind state division to cater to the need to differentiate states of brain activities. The resulting clusters corresponding to different states were then be discussed in *examination of abnormalities*, where an in-depth examination was then performed on the detected abnormalities. *Verification* checked the credibility of the conclusions drawn in the case study against the ground truth. Note that this a priori knowledge was not involved in the first two stages but only the final *verification*.

The CHB-MIT scalp EEG dataset[1] was used for this study, which was recorded simultaneously at 256 Hz with 916 h from 23 pediatric patients with severe epilepsy caused by organic lesions [42]. This study examined the EEG data of 10 patients[2] out of the 23 subjects as these consist of the same number of channels.

6.1. Blind exploration

EEG data were first divided into portions of 20 min each to view the evolution in a shorter duration rather than in a full time scale in hours. There was no overlap between the portions. For each portion, a sliding window with a length of 8 s (2048 data points) applied to segment it at a pace of 4 s. A 3-order EEG tensor (*sample* − *channel* − *frequency*) per portion was constructed after the DFT of EEG segments with a pass band of 0–50 Hz, and factor matrices were constructed by means of BF as this method excelled in extracting the latent structural information. The 1-mode factor matrix for each portion (the *sample factor matrix*) was then clustered for *blind exploration*. Multiple clusters were obtained for most portions of each patient. For a small amount of them, two clusters were obtained. Through visual inspection, no informative observations were obtained for the former cases.

In sharp contrast, significant differences could be observed in the latter cases: typical clustering results for each patient are presented in Fig. 8. In these cases, most samples were concentrated in the green cluster. The samples in the red cluster were rare that is, approximately 6.5% in all the samples in a portion, compared with those in the green cluster. The highest proportion was 9% of patient chb04 and the lowest was 4.33% of patient chb07. By tracing the samples back to the time domain, it was found that the samples in the red cluster were a continuous segment with short duration. Note that the duration time of the samples in red cluster was variant, even for one patient. They formed in a similar salient pattern and showed abnormalities in the rest.

[1] Authorized for open access at the PhysioNet website: http://physionet.org/physiobank/database/chbmit/.

[2] chb01, chb02, chb03, chb04, chb05, chb07, chb08, chb10, chb23, and chb24.

Table 3
Benchmark results on public datasets: AMI and ARI.

Dataset	Flame		Spiral		R15		Aggregation		S1		Unbalance	
Algorithms	ARI	AMI	ARI	AMI	ARI	AMI	ARI	AMI	ARI	AMI	ARI	AMI
K-means	0.451	0.396	−0.006	−0.005	0.993	0.994	0.761	0.877	0.987	0.986	1.000	1.000
DBSCAN	0.971	0.935	1.000	1.000	0.922	0.934	0.975	0.967	0.972	0.970	0.999	0.988
DPC	1.000	1.000	1.000	0.703	0.982	0.986	0.998	0.995	0.989	0.989	0.999	0.999
DPC-KNN	1.000	1.000	0.999	1.000	0.992	0.993	0.994	0.993	0.987	0.988	0.999	0.999
ADPC	1.000	1.000	1.000	1.000	0.994	0.995	1.000	1.000	0.996	0.997	1.000	0.999

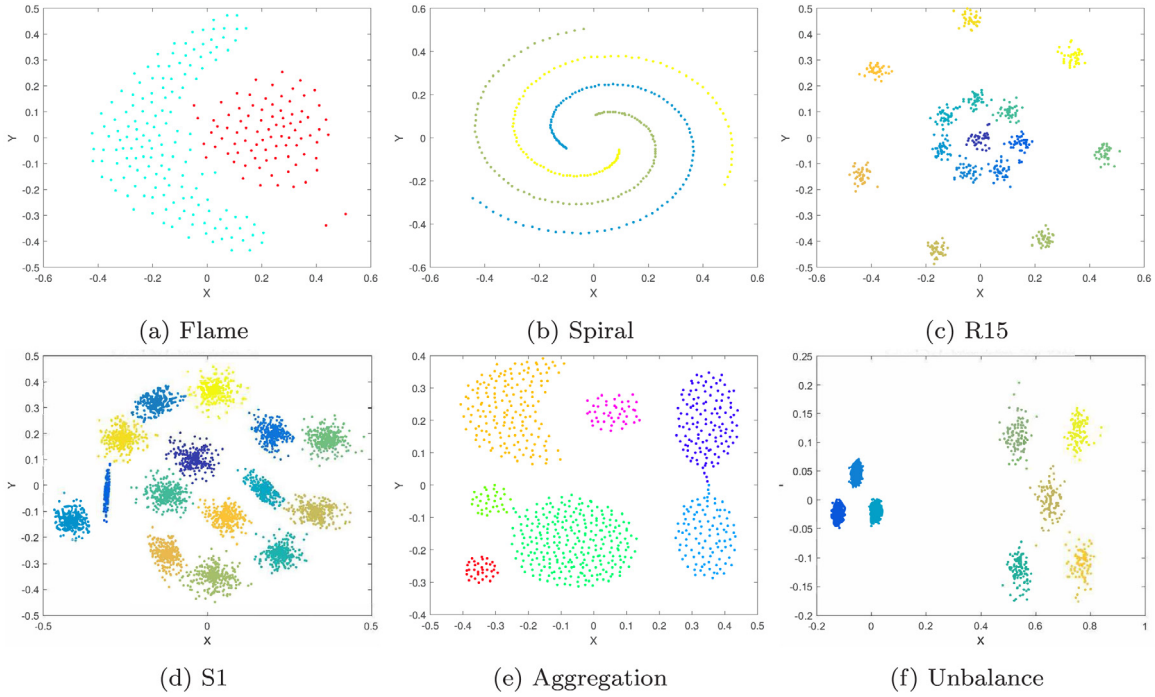

Fig. 7. Clustering results of ADPC on each dataset.

6.2. Examination of abnormalities

The samples in the red clusters were examined to determine the neurophysiological characteristics associated with the abnormalities. The key observations are as follows:

- As illustrated in Fig. 9, there is a significant difference between the samples in the two clusters. The amplitude of those in the red cluster was much larger with violent oscillations, which formed abnormalities in sharp contrast to the green cluster. In fact, this observation agrees well with the conclusions of ictal EEG samples vs. inter-ictal ones [43]. The abnormal samples in the red cluster were prone to ictal.
- Fig. 10 presents the characteristics of the samples in the red cluster in frequency and channel domains. In Fig. 10(a), there was a peak at a low frequency of approximately 2.5 Hz. In Fig. 10(b), the corresponding channel pair (F8-T8) in temporal lobe region exhibited significant neural activity. These observations provide key evidence that corresponds to epileptic seizures.

6.3. Verification

To verify the preliminary conclusions on the results obtained by the ADPC-based framework (green cluster: inter-ictal, red cluster: ictal), the labels obtained via clustering were verified against the labels (ground truth) provided by the experts with the original EEG dataset. Table 4 illustrates the confusion matrix for the sum of all patients, where Precision, Recall, F1-score, and Accuracy reached 100%, 92.49%, 96.10%, and 99.47%, respectively.

Table 4
Confusion matrix between the labels provided by the expert and the clustering labels.

	Clustering results			Precision	Recall	F1-score	Accuracy
	Stage	Ictal	Inter-ictal	(%)	(%)	(%)	(%)
Expert	Ictal	197	16				
	Inter-ictal	0	2787	100	92.49	96.10	99.47

Table 5
The clustering results of epileptic EEG data.

Patient ID	Precision (100%)	Recall (100%)	F1-score (100%)	Accuracy (100%)
chb01	100.00	84.00	91.30	98.67
chb02	100.00	100.00	100.00	100.00
chb03	100.00	100.00	100.00	100.00
chb04	100.00	100.00	100.00	100.00
chb05	100.00	83.33	90.91	98.97
chb07	100.00	81.25	89.66	99.00
chb08	100.00	96.15	98.04	99.67
chb10	100.00	94.12	96.97	99.67
chb23	100.00	85.71	92.31	98.67
chb24	100.00	100.00	100.00	100.00
Average	100.00	92.46	95.92	99.47

The clustering results for each patient are presented in Table 5. The Precision of each patient was 100%, indicating that all abnormal samples identified were ictal samples. The average Recall and F1-score of all patients' clustering results reached 92.46% and

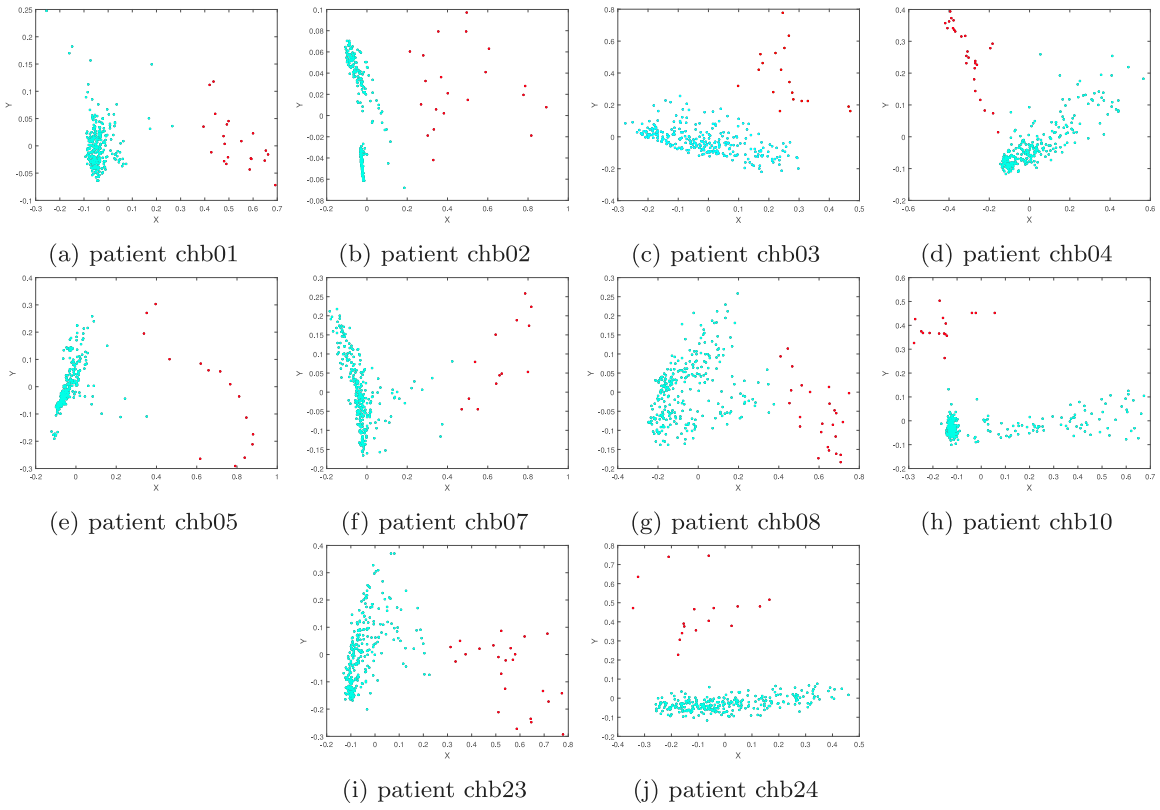

Fig. 8. Clustering results on factors of the EEG samples with each patient.

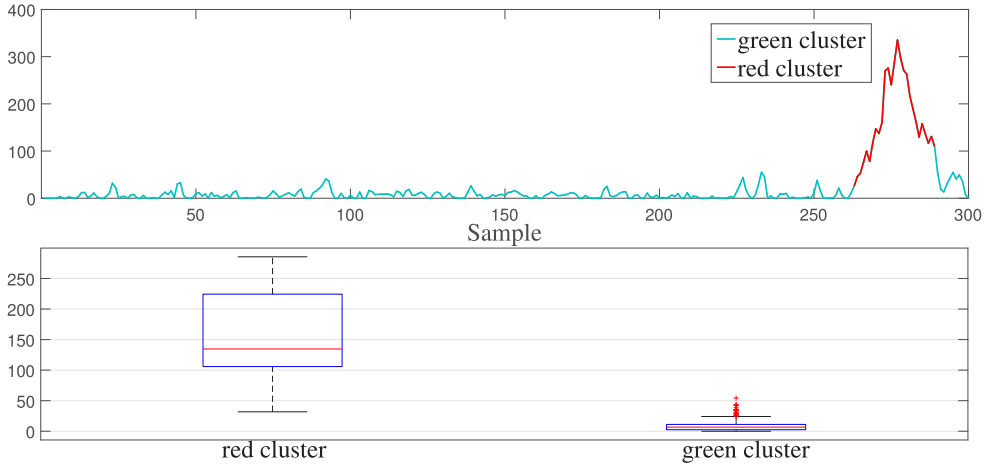

Fig. 9. Examination of abnormalities (*sample* component) in time course.

95.92%, respectively. Recall was affected by the uneven proportion of samples, and the number of ictal samples was small. The average results were calculated based on the number of patients. The results of *verification* indicate that the identification of the two clusters obtained in *blind exploration* is consistent with the preliminary conclusions in *examination of abnormalities*.

6.4. Comparison

Moreover, DPC-KNN was applied to complete the clustering task with the same EEG portions. However, the setting of parameter (p) affects the clustering results. As shown in Fig. 11 (a, b, c), when different p values were set, the clustering results were different and the result of p = 2% (F1-score = 81.82%) was better than those of p = 1% and 3% (F1-score = 76.19%) for chb08 patients.

In addition, the appropriate selection of cluster centers in DPC-KNN was not easy because of the manual determination via Decision Graph. As shown in Fig. 11 (d, e, f), the three points in the upper right corner all had the possibility of becoming the cluster centers, and different results were obtained by determining different cluster centers from the Decision Graph. The problem of ambiguous selection of cluster centers also emerged with patient chb03. As shown in Fig. 12, there were four close points in the upper right corner of the Decision Graph, which probably led to the selection of four cluster centers. Even assuming that the number of known clusters was 2, it remains unclear which two cluster centers to choose.

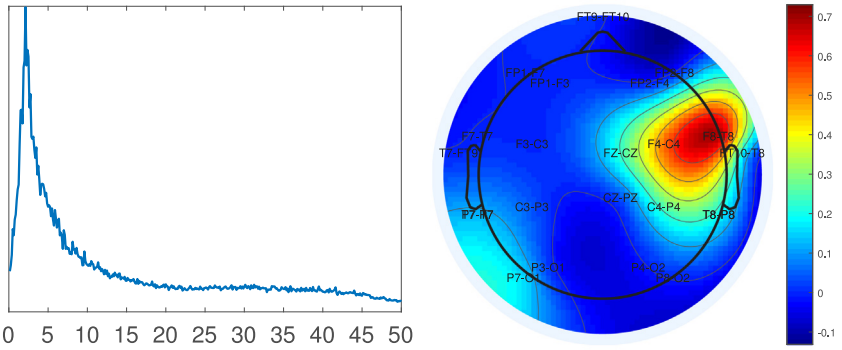

(a) frequency component of red cluster (b) channel component of red cluster

Fig. 10. Examination of abnormalities in frequency and channel domains.

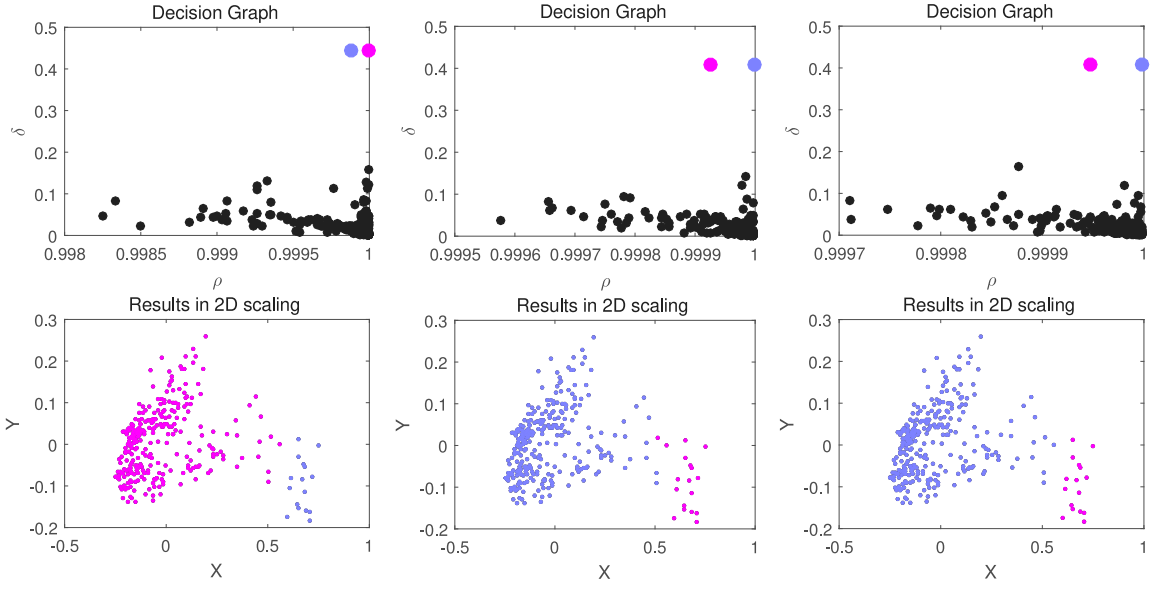

(a) chb08's result (1), p=1% (b) chb08's result (2), p=2% (c) chb08's result (3), p=3%

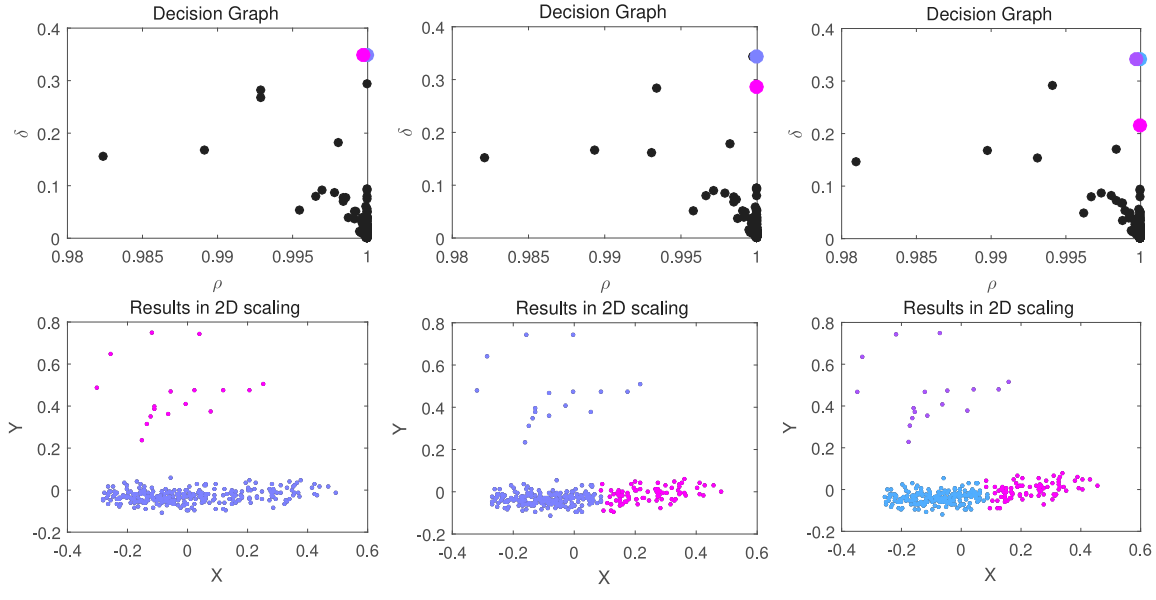

(d) chb24's result (1) (e) chb24's result (2) (f) chb24's result (3)

Fig. 11. DPC-KNN Decision Graph and clustering results of patient chb08 and chb24.

Table 6
The accuracy for seizure state detection (seizure and non-seizure).

Authors	Approaches included	Accuracy (100%)
Chen et al. [44]	G-HALS + Multi-layer perception (MLP)	99.35
Tang et al. [35]	Bayesian tensor factorization (BTF) + Multi-layer perception (MLP)	99.52
Alickovic et al. [45]	Wavelet packet decomposition + Random forest (RF)	100.00
Ke et al. [46]	Maximal information coefficient (MIC) + Convolutional neural networks (CNN)	98.13
Yuan et al. [47]	Autoencoder + Wavelet-based context learning	94.37
Proposed method	EEG exploratory analysis framework	99.47

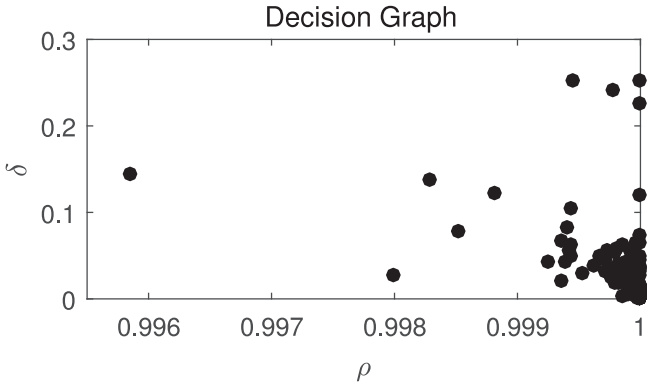

Fig. 12. DPC-KNN Decision Graph of patient chb03.

Overall, the case study indicated that the ADPC-based framework holds the potential for exploratory EEG analysis (detection of epileptic seizure) in comparison with experts' labeling. This helped in the discovery of abnormal neural activity .

For the CHB-MIT epileptic EEG dataset, the methods proposed in [35,44–47] were compared as baselines in terms of the accuracy of seizure detection. The details of these methods are presented in Table 6. As shown in Table 6, the proposed framework achieves the same expected performance as most state-of-the-art methods. It should also be noted that these methods [45–47] were designed specifically for epileptic seizure analysis. Furthermore, the MLP model in Ref. [35,44] is a supervised method that requires training data with labels for training the model, but the proposed method did not. Note that ADPC is an unsupervised method without the need for labeling, it was not surprising that its performance in terms of "classification" did not reach the precision achieved by excellent supervised methods but was already close enough [44,45] .

6.5. Discussions

By combining the feature extraction method which can extract the maximum amount of information without knowledge, the ADPC-based framework complemented the existing supervised and semi-supervised methods in EEG analysis. The framework could explore the internal structure and pattern of pathological EEG via clustering approach.

Neuro-scientists and practitioners were then able to complete the initial exploration of abnormalities in EEG with constraints previously mandatory removed, such as labels and background information of the subjects, by the ADPC-based framework. Meanwhile, they also could choose specific clusters of the clustering results for in-depth analysis or support the classification with a (semi-)supervised method.

7. Conclusions

Inspired by the urgent need in the field of clustering to automate the process of finding appropriate cluster centers and determining their scope of influence, this study fostered an adaptive solution (ADPC) based on the density peaks clustering theory. In particular, the solution aimed to tackle the challenges in the exploratory analysis of bio-signals using EEG as a case study.

ADPC enabled adaptive selection of the cutoff distance with an optimization function constructed with the Gini index to measure the uncertainty of the target dataset. An extended PSA was developed to obtain the optimal cutoff distance value. ADPC supported the automatic determination of the cluster centers. It automatically constructed a set of cluster centers by jointly ranking the local density and relative distance and then fine-tuning the set by balancing the intra-set independence and the tendency as a center against extra-set competitors.

Benchmarks on public datasets indicated ADPC's superiority of adaptability to various datasets and effectiveness against the mainstream counterparts in terms of ARI and AMI. The case study of the ADPC-based framework on epileptic EEG indicated that (1) the framework achieved an average on Precision, Recall, and F1-score of 100%, 92.46%, and 95.92%, respectively, in seizure detection involving no priori information, and (2) the key observations revealed through clustering well match the expert's conclusions.

ADPC enabled fully automated adaptive clustering based on the target dataset without the need for human intervention or an empirical setting of key parameters. The ADPC empowered the exploratory analysis of EEG, which was previously a well-known problem in the community of bio-signal processing. The resulting framework on its top could find abnormal neural activities from EEG without explicit a priori knowledge of the subjects under examination as the classification models do.

Overall, ADPC holds potential in exploratory analysis of bio-signals in general, as it operated independently in the course of data exploration.

Declaration of competing interest

The authors declare that they have no known competing financial interests or personal relationships that could have appeared to influence the work reported in this paper.

Acknowledgments

This work was supported in part by Scientific and Technological Innovation 2030, China (No. 2021ZD0204300), the National Natural Science Foundation of China (Nos. 62172304, 61977027), and Science & Technology Major Project of Hubei Province, China (Next-Generation AI Technologies, No. 2021BEA159). We would like to show our deepest gratitude to Ms. Siwei Chen for providing the original ideas for this work and our special thanks to Prof. Xiaoli Li, Mr. Lei Zhang, and Dr. Hengjin Ke for their assistance through all stages in this study.

References

[1] H.-P. Kriegel, P. Kröger, A. Zimek, Clustering high-dimensional data: A survey on subspace clustering, pattern-based clustering, and correlation clustering, Acm Trans. Knowl. Discov. Data (TKDD) 3 (1) (2009) 1–58.

[2] B.A. Pimentel, A.C. de Carvalho, A meta-learning approach for recommending the number of clusters for clustering algorithms, Knowl.-Based Syst. 195 (2020) 105682.
[3] S. Ma, L. Zhang, W. Hu, Y. Zhang, J. Wu, X. Li, Self-representative manifold concept factorization with adaptive neighbors for clustering, in: IJCAI International Joint Conference on Artificial Intelligence, 2018.
[4] P. Masulli, F. Masulli, S. Rovetta, A. Lintas, A.E. Villa, Fuzzy clustering for exploratory analysis of EEG event-related potentials, IEEE Trans. Fuzzy Syst. 28 (1) (2019) 28–38.
[5] A. Arh, B. As, C. Yz, Epilepsy seizure detection using complete ensemble empirical mode decomposition with adaptive noise, Knowl.-Based Syst. 191 (2020) 105333.
[6] C. Dai, J. Wu, D. Pi, S.I. Becker, B. Johnson, Brain EEG time-series clustering using maximum-weight clique, IEEE Trans. Cybern. PP (99) (2020) 1–15.
[7] S. Mccloskey, B. Jeffries, I. Koprinska, C.B. Miller, R.R. Grunstein, Data-driven cluster analysis of insomnia disorder with physiology-based qEEG variables, Knowl.-Based Syst. 183 (Nov.1) (2019) 104863.1–104863.11.
[8] C. Dai, J. Wu, D. Pi, L. Cui, B. Johnson, S.I. Becker, Electroencephalogram signal clustering with convex cooperative games, IEEE Trans. Knowl. Data Eng. PP (2021).
[9] J. Deng, J. Guo, Y. Wang, A novel k-medoids clustering recommendation algorithm based on probability distribution for collaborative filtering, Knowl.-Based Syst. 175 (JUL.1) (2019) 96–106.
[10] S.S. Khan, A. Ahmad, Cluster center initialization algorithm for k-means clustering, Pattern Recognit. Lett. 25 (11) (2004) 1293–1302.
[11] C. Bouveyron, S. Girard, C. Schmid, High-dimensional data clustering, Comput. Statist. Data Anal. 52 (1) (2007) 502–519.
[12] A.K. Jain, Data clustering: 50 years beyond k-means, Pattern Recognit. Lett. 31 (8) (2010) 651–666.
[13] J. Sander, M. Ester, H.-P. Kriegel, X. Xu, Density-based clustering in spatial databases: The algorithm gdbscan and its applications, Data Min. Knowl. Discov. 2 (2) (1998) 169–194.
[14] M. Ester, H.-P. Kriegel, J. Sander, X. Xu, et al., A density-based algorithm for discovering clusters in large spatial databases with noise, in: KDD, Vol. 96, 1996, pp. 226–231.
[15] Y. Cheng, Mean shift, mode seeking, and clustering, IEEE Trans. Pattern Anal. Mach. Intell. 17 (8) (1995) 790–799.
[16] A. Rodriguez, A. Laio, Clustering by fast search and find of density peaks, Science 344 (6191) (2014) 1492–1496.
[17] Y. Chen, X. Hu, W. Fan, L. Shen, H. Li, Fast density peak clustering for large scale data based on kNN, Knowl.-Based Syst. 187 (2020) 104824.
[18] J. Xu, G. Wang, T. Li, W. Deng, G. Gou, Fat node leading tree for data stream clustering with density peaks, Knowl.-Based Syst. 120 (2017) 99–117.
[19] U. Rajendra Acharya, H. Fujita, Vidya K. Sudarshan, Shreya Bhat, Joel E.W. Koh, Application of entropies for automated diagnosis of epilepsy using EEG signals: A review, Knowl.-Based Syst. 88 (2015) 85–96.
[20] R. Xu, D. Wunsch, Survey of clustering algorithms, IEEE Trans. Neural Netw. 16 (3) (2005) 645–678.
[21] A. Fahad, N. Alshatri, Z. Tari, A. Alamri, I. Khalil, A.Y. Zomaya, S. Foufou, A. Bouras, A survey of clustering algorithms for big data: Taxonomy and empirical analysis, IEEE Trans. Emerg. Top. Comput. 2 (3) (2014) 267–279.
[22] X. Xu, S. Ding, Z. Shi, An improved density peaks clustering algorithm with fast finding cluster centers, Knowl.-Based Syst. 158 (2018) 65–74.
[23] K.G. Flores, S.E. Garza, Density peaks clustering with gap-based automatic center detection, Knowl.-Based Syst. 206 (2020) 106350.
[24] M. Du, S. Ding, H. Jia, Study on density peaks clustering based on k-nearest neighbors and principal component analysis, Knowl.-Based Syst. 99 (2016) 135–145.
[25] J. Jiang, D. Hao, Y. Chen, M. Parmar, K. Li, GDPC: Gravitation-based density peaks clustering algorithm, Physica A 502 (2018) 345–355.
[26] J. Wang, Y. Zhang, X. Lan, Automatic cluster number selection by finding density peaks, in: 2016 2nd IEEE International Conference on Computer and Communications (ICCC), IEEE, 2016, pp. 13–18.
[27] R. Bie, R. Mehmood, S. Ruan, Y. Sun, H. Dawood, Adaptive fuzzy clustering by fast search and find of density peaks, Pers. Ubiquitous Comput. 20 (5) (2016) 785–793.
[28] S.A. Alshebeili, A. Sedik, B. Abd El-Rahiem, T.N. Alotaiby, G.M. El Banby, H.A. El-Khobby, M.A. Ali, A.A. Khalaf, F.E. Abd El-Samie, Inspection of EEG signals for efficient seizure prediction, Appl. Acoust. 166 (2020) 107327.
[29] P.A. Bizopoulos, D.G. Tsalikakis, A.T. Tzallas, D.D. Koutsouris, D.I. Fotiadis, EEG epileptic seizure detection using k-means clustering and marginal spectrum based on ensemble empirical mode decomposition, in: 13th IEEE International Conference on BioInformatics and BioEngineering, IEEE, 2013, pp. 1–4.
[30] S. Wang, W. Gan, D. Li, D. Li, Data field for hierarchical clustering, Int. J. Data Warehousing Mining (IJDWM) 7 (4) (2011) 43–63.
[31] R. Michael, L.V. Torczon, Pattern search methods for linearly constrained minimization, SIAM J. Optim. 10 (3) (2000) 917–941.
[32] S. Wang, S. Wang, H. Yuan, Q. Li, J. Geng, Y. Yu, Clustering by differencing potential of data field, Computing 100 (4) (2018) 403–419.
[33] G. Giachetta, L. Mangiarotti, et al., Advanced Classical Field Theory, World Scientific, 2009.
[34] S. Wang, D. Wang, Elmdf: A new classification algorithm based on data field, in: 2014 IEEE International Conference on Bioinformatics and Biomedicine (BIBM), IEEE, 2014, pp. 28–33.
[35] Y. Tang, D. Chen, L. Wang, A.Y. Zomaya, J. Chen, H. Liu, Bayesian tensor factorization for multi-way analysis of multi-dimensional EEG, Neurocomputing 318 (2018) 162–174.
[36] L. Fu, E. Medico, P flame, a novel fuzzy clustering method for the analysis of dna microarray data, BMC Bioinformatics 8 (1) (2007) 3.
[37] H. Chang, D.-Y. Yeung, Robust path-based spectral clustering, Pattern Recognit. 41 (1) (2008) 191–203.
[38] C.J. Veenman, M.J.T. Reinders, E. Backer, A maximum variance cluster algorithm, IEEE Trans. Pattern Anal. Mach. Intell. 24 (9) (2002) 1273–1280.
[39] A. Gionis, H. Mannila, P. Tsaparas, Clustering aggregation, Acm Trans. Knowl. Discov. Data (TKDD) 1 (1) (2007) 4–es.
[40] P. Fränti, O. Virmajoki, Iterative shrinking method for clustering problems, Pattern Recognit. 39 (5) (2006) 761–775.
[41] M. Rezaei, P. Fränti, Set matching measures for external cluster validity, IEEE Trans. Knowl. Data Eng. 28 (8) (2016) 2173–2186.
[42] A.H. Shoeb, J.V. Guttag, Application of machine learning to epileptic seizure detection, in: Proceedings of the 27th International Conference on Machine Learning (ICML-10), 2010, pp. 975–982.
[43] U.R. Acharya, S.V. Sree, G. Swapna, R.J. Martis, J.S. Suri, Automated EEG analysis of epilepsy: a review, Knowl.-Based Syst. 45 (2013) 147–165.
[44] D. Chen, Y. Tang, H. Zhang, L. Wang, X. Li, Incremental factorization of big time series data with blind factor approximation, IEEE Trans. Knowl. Data Eng. 33 (2) (2021) 569–584.
[45] E. Alickovic, J. Kevric, A. Subasi, Performance evaluation of empirical mode decomposition, discrete wavelet transform, and wavelet packed decomposition for automated epileptic seizure detection and prediction, Biomed. Signal Process. Control 39 (2018) 94–102.
[46] H. Ke, D. Chen, X. Li, Y. Tang, T. Shah, R. Ranjan, Towards brain big data classification: Epileptic EEG identification with a lightweight vggnet on global mic, IEEE Access 6 (2018) 14722–14733.
[47] Ye Yuan, Guangxu Xun, Kebin Jia, Aidong Zhang, A multi-view deep learning framework for EEG seizure detection, IEEE J. Biomed. Health Inf. 23 (1) (2018) 83–94.